

Capturing positive utilities during the estimation of recursive logit models: A prism-based approach

Yuki Oyama^{a,*}

^a*Shibaura Institute of Technology, Department of Civil Engineering*

Abstract

Although the recursive logit (RL) model has been recently popular and has led to many applications and extensions, an important numerical issue with respect to the evaluation of value functions remains unsolved. This issue is particularly significant for model estimation, during which the parameters are updated every iteration and may violate the model feasible condition. To solve this numerical issue, this paper proposes a prism-constrained RL (Prism-RL) model that implicitly restricts the path set by the prism constraint defined based upon a state-extended network representation. Providing a set of numerical experiments, we show that the Prism-RL model succeeds in the stable estimation regardless of the initial and true parameter values and is able to capture positive utilities. In the real application to a pedestrian network, we found the positive effect of street green presence on pedestrians. Moreover, the Prism-RL model achieved a higher goodness of fit than the RL model, implying that the Prism-RL model can also describe more realistic route choice behavior.

Keywords: Route choice analysis, recursive logit, prism constraint, pedestrian, GPS, urban design

1. Introduction

Recursive logit (RL) models, which are derived based upon the Markov decision process, provide a computationally efficient way of modeling route choice behavior in the sense that they do not require path enumeration (Akamatsu, 1996; Fosgerau et al., 2013). However, the evaluation of value functions required in the computation of such models are still challenging. The value function may diverge when the network contains cycles, depending on the utility value of the elemental choice (e.g., node or link transition), as shown in the illustrative examples of Oyama and Hato (2017, 2019). This numerical problem is in particular significant in model estimation. During the estimation process, the model parameters that decide the utility values are updated with every iteration. Even if the initial and true parameters are feasible solutions, parameters in the middle of the estimation may violate the model feasibility condition and cause divergence of the value functions. To somehow avoid this numerical issue, studies in the literature included only negative utilities (e.g., travel time or distance) and added a negative fixed penalty term for u-turns in the utility function (e.g., Fosgerau et al., 2013; Mai et al., 2015). These ad hoc manipulations imply, however, the limitation of the applicability of the RL models. Recursive modeling of behavior is a general framework and its application is not limited to just route choice behavior, but also to various types of sequential decision making, such as destination sequences (Gao and Schmöcker, 2021) or mode chains (de Freitas et al., 2019). The possible impacts of the urban/transport planning projects to be evaluated are not limited to negative ones. In recent urban design projects, for example, planners make better places to improve the walkability of city centers (e.g., Mehta, 2008; Mueller et al., 2020), and the RL model can be a useful tool for evaluating possible positive impacts on pedestrian behavior. Therefore, to increase the practical

*Corresponding author

Email address: oyama@shibaura-it.ac.jp (Yuki Oyama)

applicability of the RL models, it is important to solve their numerical issue and enable capturing positive variable impacts on utility.

This study is the first to propose a method of estimating a recursive logit model without any constraint on parameters or utilities, based on the prism-based path set restriction of [Oyama and Hato \(2019\)](#). The path set restriction method was proposed for the Markovian traffic assignment and redefines the value functions on a state-extended network, which solves the divergence of the value function without the loss of operationality and efficiency (i.e., the implicit path enumeration) of the RL model. However, its application to model estimation has not been presented. In this study, we propose a novel RL model based on the prism-based path restriction method (Prism-RL) and show its potential to capture positive utilities in the model estimation. We provide a set of numerical experiments to examine the model properties in comparison with the RL model. As a real case study, we consider an urban pedestrian network where pedestrians walk in a city center and may perceive not only negative utilities (i.e. travel costs), but also positive ones such as the attractiveness of the streets.

This paper is structured as follows. Section 2 reviews the RL model and its recent advances, as well as its numerical problems. Then, in Section 3, we propose the Prism-RL model. Section 4 provides two types of results: one uses simulated observations, and the other shows a real case study of pedestrian route choice analysis. Finally, we conclude the study in Section 5. The appendices further provide characteristics of the network and behavioral data used in the analysis, computational reports, and a mathematical proposition.

2. Recursive logit model: Literature review and challenge

This section shortly reviews the RL model ([Fosgerau et al., 2013](#)) and its recent advances, and we also discuss its numerical problem.

Consider a connected directed graph $G = (N, L)$ that is not assumed acyclic, where N is the set of nodes and L is the set of links. The RL model describes a route choice behavior by a sequence of elemental state/action choices, based on a deterministic Markov decision process with i.i.d. Gumbel distributed rewards ([Ziebart et al., 2008](#); [Rust, 1987](#)). Note that, depending on the state definition, a RL model can be either node-based or link-based. A node-based RL model provides a simpler description of route choice behavior with efficient computation and is often implemented in traffic assignment models (e.g., [Akamatsu, 1996](#); [Oyama et al., 2022](#)). In contrast, a link-based model describes a transition between two links, i.e. the geometric relationships of three nodes, and may capture more flexible mechanisms of behavior. For this reason, studies in the context of discrete choice analysis often use a link-based RL model (e.g., [Fosgerau et al., 2013](#); [Mai et al., 2015](#)), and we also used a link-based model in the case studies in Section 4.

A traveler at state k is assumed to choose the next state (i.e., action) a that maximizes the sum of instantaneous utility $u(a|k)$ and the expected downstream utility $V^d(a)$ to destination (absorbing state) d . The utility $u(a|k)$ is further decomposed into the deterministic component $v(a|k)$ and the error component $\epsilon(a|k)$. The expected utility $V^d(k)$ is the value function of state k that is formulated via Bellman's equation:

$$V^d(k) \equiv \mathbb{E} \left[\max_{a \in A(k)} \{v(a|k) + V^d(a) + \mu \epsilon(a|k)\} \right], \quad (1)$$

where $A(k)$ is the set of states connected to (i.e., available actions for) state k , and μ is the scale of $\epsilon(a|k)$. With the distributional assumption $\epsilon(a|k) \stackrel{iid}{\sim} \text{Gumbel}(0, \mu)$ and by taking exponentials, (1) reduces to

$$e^{\frac{1}{\mu} V^d(k)} = \sum_{a \in A(k)} e^{\frac{1}{\mu} \{v(a|k) + V^d(a)\}}, \quad (2)$$

which is a system of linear equations. In the matrix form, (2) is compactly written as

$$\mathbf{z}^d = \mathbf{M}\mathbf{z}^d + \mathbf{b}^d \Leftrightarrow \mathbf{z}^d = (\mathbf{I} - \mathbf{M})^{-1}\mathbf{b}^d \quad (3)$$

where $z_k^d = e^{\frac{1}{\mu}V^d(k)}$, $M_{ka} = \delta(a|k)e^{\frac{1}{\mu}v(k|a)}$, and $\delta(a|k)$ is the state-action incidence. b_k^d equals one if $k = d$ and zero otherwise. Finally, the RL model describes the choice probability of a path (i.e., state sequence) $\sigma = [k_1, \dots, k_J]$ by a product of elemental choice probabilities:

$$P(\sigma) = \prod_{j=1}^{J-1} p^d(k_{j+1}|k_j) = \prod_{j=1}^{J-1} \frac{e^{\frac{1}{\mu}\{v(k_{j+1}|k_j) + V^d(k_{j+1})\}}}{\sum_{a \in A(k_j)} e^{\frac{1}{\mu}\{v(a|k_j) + V^d(a)\}}}. \quad (4)$$

Note that the equivalence of (4) to the multinomial logit (MNL)-type route choice model with the unrestricted path set has been proved (Akamatsu, 1996; Fosgerau et al., 2013). We refer to Fosgerau et al. (2013) for more details of the RL model.

Because of its computational efficiency, the RL model has been recently popular and extended to a variety of variants, such as a nested logit model (Mai et al., 2015), the network multivariate extreme value (NMEV) model (Mai, 2016), a mixture model (Mai et al., 2018), incorporation of the spatial discount factor (Oyama and Hato, 2017), travel information (de Moraes Ramos et al., 2020), and network uncertainty (Mai et al., 2021). Oyama and Hato (2018) and van Oijen et al. (2020) proposed network-free parameter estimation methods which are based on raw trajectory data of GPS locations and WiFi traces, respectively. The mathematical equivalence of the RL model with the Markovian traffic assignment (Akamatsu, 1996, 1997; Baillon and Cominetti, 2008) is also discussed, and the advanced model (Oyama et al., 2022) or applications to the field of machine learning (Saerens et al., 2009; Kivimäki et al., 2020) have been recently studied.

However, the RL model still has a fundamental numerical issue to be addressed: the existence of its solution depends on the structure of the network, the magnitude of utility, and the values of the model parameters. When the network contains cycles, the value function may diverge depending on the model parameters. Mathematically, the necessary and sufficient condition to solve (3) is that the spectral radius $\rho(\mathbf{M})$, i.e., the maximum absolute of the eigenvalue, of the matrix \mathbf{M} is strictly smaller than one (Oyama and Hato, 2017, 2019). To somehow satisfy this condition, studies on the RL models often include only negative variable effects and/or add a fixed large penalty for u-turns (e.g., Fosgerau et al., 2013; Mai et al., 2015). However, there is no guarantee that such ad hoc manipulations of the utility function always resolve the numerical issue. Oyama and Hato (2017, 2019) also showed in numerical experiments that the value function can diverge even when only negative variable effects are contained in the utility function. Incorporating the discount factor may alleviate the problem (Oyama and Hato, 2017), but a large discount (i.e. a small discount factor) of the value function does not seem very realistic in ordinary networks on a real scale.

Recently, in the traffic assignment field, Oyama and Hato (2019) proposed a way to solve the numerical issue of value function evaluation for the RL model. They introduce a prism constraint to the network and restrict the path set while retaining the implicit path enumeration. The authors also applied the method to Markovian traffic equilibrium and showed that the incorporation of the prism constraint relaxed the excessive cyclic flows as well as made the problem solvable regardless of the network conditions. In the paper, the constraint parameter (called choice stage constraint) defining the prism was arbitrarily given. It is, however, ideal to define the parameter based on real observations. Furthermore, the applicability of the prism-based approach to model estimation has not yet been validated. The numerical issue regarding the value function may be more significant in the case of the estimation, during which the model parameters are updated every iteration. The model can become infeasible during the estimation, even if the initial and true parameters are feasible solutions. In particular, when we want to deal with many parameters

or capture positive variable effects, it is not likely to succeed in estimating the RL model without any numerical issue. Thus, it is important to validate the prism-based approach for the estimation of the RL models.

3. Methodology

This section presents the Prism-RL model, which is the RL model based on the prism-based path set restriction method proposed by Oyama and Hato (2019). We also present its behavioral interpretation and model estimation method.

3.1. Prism-based Path Set Restriction

A state-extended network is constructed based on the spatial network G , where a state s is defined based on a pair of *choice stage* t and space (a node or link) k , that is, $s = (t, k)$. A choice stage is the timing of a traveller's decision making and does not indicate a time. We assume that instantaneous utility $v(a|k)$ does not vary by choice stage, which means that our approach is not a dynamic model¹. Based on the extended network, a choice stage constraint T is further introduced. T means the maximum number of choices a traveler can experience on the network, whose interpretation differs from the definition of the original network (see Table 1 of Oyama and Hato, 2019). Under the constraint, a traveler who wants to travel to the destination d must arrive there at or before the choice stage T , that is, her terminal state is always $s_T = (T, d)$. We use this fact to reduce the size of states in the network and restrict the set of feasible paths.

Let $D^d(k)$ denote the minimum number of steps (i.e., choice stages) to take from k to d , which can be computed with a shortest path algorithm on G . The existence condition $I^d(s)$ of state $s = (t, k)$ is then defined as

$$I^d(t, k) = \begin{cases} 1, & \text{if } D^d(k) \leq T - t \\ 0, & \text{otherwise.} \end{cases} \quad \forall t \in \{0, \dots, T-1\} \quad (5)$$

which means that a traveler is allowed to be in space k at only t that satisfies $I^d(t, k) = 1$. The state set S_t^d at choice stage t thus reduces to $S_t^d \equiv \{s = (t, k) | I^d(s) = 1\}$. Moreover, a state transition is possible only when two states exist and are spatially connected, i.e., the state connection condition $\Delta^d(s'|s) = \Delta_t^d(a|k)$ between states $s = (t, k)$ and $s' = (t+1, a)$ is

$$\Delta_t^d(a|k) = I^d(t, k) \delta(a|k) I^d(t+1, a). \quad (6)$$

The set of edges (connected pairs of states) E_t^d is also restricted to $E_t^d \equiv \{(s, s') = ((t, k), (t+1, a)) | \Delta^d(s'|s) = 1\}$. The constraint Δ implies that the set of spaces available to a traveler varies by choice stage t even if she is in the same space. Thus, feasible paths must include only states in the reduced network. The set of paths that a traveler can choose results in the formation of a prism (Hägerstrand, 1970), which exhibits a sphere of possible behavior of a traveler in the state-extended network.

Two remarks are in order here. First, the choice stage constraint T shall be defined based upon each destination ($T \equiv T_d$) or each origin-destination (OD) pair ($T \equiv T_{od}$). The information from real observations, such as detour characteristics or the maximum number of choice stages in a path, can be utilized for the decision, for which we later show an example in the real case study of Section 4.2. Second, while we have discussed above the prism that has only a vertex of the final state (T, d) , it can be defined based also upon the initial state $s_0 = (0, o)$ where o is the

¹This study focuses on a static model for the comparison with the original RL model, while the extension to a time-space network description is straightforward (Oyama and Hato, 2016)

origin. In this case, an additional constraint is required for the existence of the state, and (5) is replaced by

$$I^{od}(t, k) = \begin{cases} 1, & \text{if } D^d(k) \leq T - t, D^o(k) \leq t \\ 0, & \text{otherwise.} \end{cases} \quad \forall t \in \{0, \dots, T-1\} \quad (7)$$

where $D^o(k)$ denotes the minimum number of steps to take from o to k . This doubly constrained prism approach describes a more precise behavioral sphere and can reduce the network states to consider, but the procedure has to be repeated as many times as the number of OD pairs, which may be computationally expensive in a large-scale network.

3.2. Prism-Constrained RL Model

We then introduce the prism-constrained RL (Prism-RL) model, which is a RL model whose path set is restricted by the prism constraint of Section 3.1. The main difference from the original RL model is that the Prism-RL model defines the value function $V^d(s) = V^d(t, k)$ for each state $s \in S \equiv \{S_0, \dots, S_T\}$ in the extended network. That is, the value function $V^d(t, k)$ is the evaluation function of the prism defined based upon the current state (t, k) and the final state (T, d) , and it may take different values by choice stages, i.e., $V^d(t, k) \neq V^d(t', k)$ (Fig. 1).

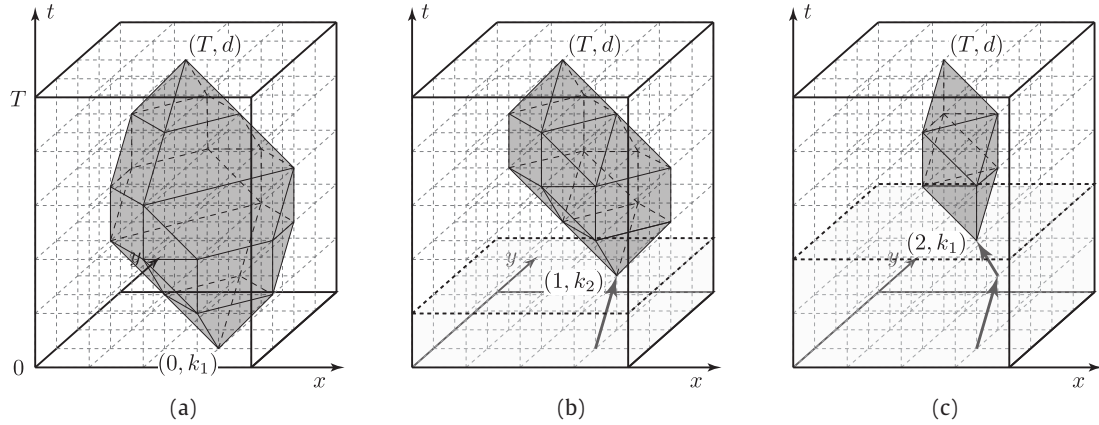


Figure 1: Prism representing the restricted set of states conditional on each of current states (a) $(0, k_1)$, (b) $(1, k_2)$, and (c) $(2, k_1)$, where the choice stage constraint is $T = 5$. The value function $V^d(s)$ evaluates all the feasible paths within the prism and thus takes different values by choice stages even in the same space; in this example, the panels (a) and (c) illustrate that $V^d(0, k_1) \neq V^d(2, k_1)$. Note that this figure shows a doubly-constrained case.

As the result, (2) and (3) of the RL model are replaced by

$$e^{\frac{1}{\mu} V^d(t, k)} = \sum_{a \in A(k)} \Delta_t^d(a|k) e^{\frac{1}{\mu} \{v(a|k) + V^d(t+1, a)\}} \quad (8)$$

and

$$\mathbf{z}_t^d = (\Delta_t^d \circ \mathbf{M}) \mathbf{z}_{t+1}^d + \mathbf{b}^d \quad (9)$$

where $\mathbf{z}_t^d(k) = e^{\frac{1}{\mu} V^d(t, k)}$. Thanks to the prism constraint and the state-specific definition of the value function, (9) can be solved with a simple backward calculation with T iterations:

Step 1: Define the final state (T, d) . Compute \mathbf{D}^d , \mathbf{I}^d , and Δ^d .

Step 2: Initialize $\mathbf{z}_T^d(d) = 1, \forall t \in \{0, \dots, T\}$. Set $t = T$, and $\mathbf{z}_T^d(k) = 0, \forall k \neq d$.

Step 3: Set $t = t - 1$. Calculate \mathbf{z}_t^d with (9).

Step 4: Finish the calculation if $t = 0$, and go back to *Step 3* otherwise.

We no longer need to solve the linear system (3), and the solution always exists regardless of the network structure or the utility specification. Moreover, the method does not depend on the linearity of the model. It is also applicable to nonlinear models, such as the nested RL model (Mai et al., 2015) and the discounted RL model (Oyama and Hato, 2017). We refer the reader to Oyama and Hato (2019) for a more detailed discussion of the computational properties and nonlinear formulations of the Prism-RL model.

Having defined the value function of the Prism-RL model, we then obtain the choice probability $p^d(s'|s) = p_t^d(a|k)$ of state $s' = (t+1, a)$ given a current state $s = (t, k)$ as

$$p_t^d(a|k) = \frac{\Delta_t^d(a|k) e^{\frac{1}{\mu} \{v(a|k) + V^d(t+1, a)\}}}{\sum_{a' \in A(k)} \Delta_t^d(a'|k) e^{\frac{1}{\mu} \{v(a'|k) + V^d(t+1, a')\}}}. \quad (10)$$

where we have the prism constraint $\Delta_t^d(a|k)$, meaning that no state transition going outside the prism is allowed even if the two states are spatially connected (Fig.2).

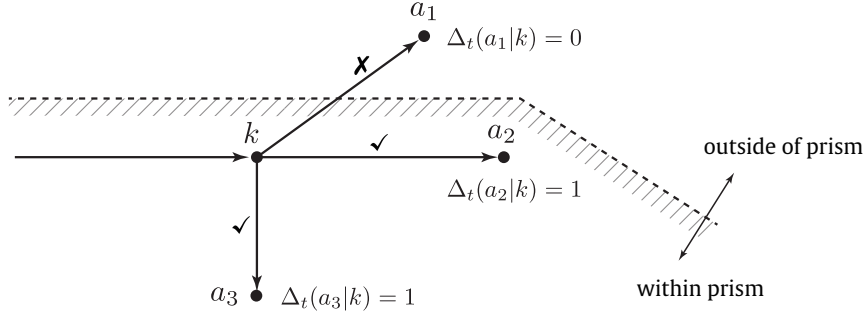


Figure 2: Route choice behavior constrained by the prism: In this example, node k is connected to three nodes $A(k) = \{a_1, a_2, a_3\}$, but state $(t+1, a_1)$ is outside of the prism, i.e., $I(t+1, a_1) = 0$. At node k and choice stage t , therefore, the choice of a_1 is violated ($\Delta_t(a_1|k) = 0$), and only the transitions to a_2 or a_3 are allowed ($\Delta_t(a_2|k) = \Delta_t(a_3|k) = 1$).

3.3. Path Translation and Model Estimation

The parameters of the Prism-RL model are estimated by the maximum likelihood estimation. Assume that we have route choice observations $\sigma_n = [k_0, \dots, k_{J_n}]$, $n \in \{1, \dots, N\}$. We set the choice stage constraint T so that it is equal to or larger than $\bar{J} \equiv \max_n J_n$. We then translate the observations into those for the Prism-RL model, i.e., $\sigma_n^* = [(0, k_0), \dots, (J_n, d_n), (J_n + 1, d_n), \dots, (T, d_n)]$, where d_n is the destination of σ_n and $k_{J_n} = \dots = k_T = d_n$. This translation does not change the nature of the data and its behavioral interpretation. The log-likelihood function of the Prism-RL model is

$$\begin{aligned} LL(\beta; \sigma^*) &\equiv \log \prod_{n=1}^N P(\sigma_n) \\ &= \sum_{n=1}^N \sum_{t=0}^{T-1} \log p_t^{d_n}(k_{t+1}|k_t) \\ &= \frac{1}{\mu} \sum_{n=1}^N \sum_{t=0}^{T-1} [v(k_{t+1}|k_t) + V^{d_n}(t+1, k_{t+1}) - V^{d_n}(t, k_t)] \end{aligned} \quad (11)$$

where β is the vector of model parameters, and $v(a|k) = v(x_{a|k}, \beta)$ is a function of β and a vector of observed attributes $x_{a|k}$ of space pair (k, a) . The scale μ is fixed to one in this study. To solve the maximization problem of (11), we applied the nested fixed point (NFXP) algorithm (Rust, 1987), in which the evaluation of the value function is performed every time the parameter is updated. Parameter search is performed by a Newton-type nonlinear optimization algorithm.

4. Results

In this section, we first present numerical experiments using observations simulated in the Sioux Falls network. In the experiments, we validate the parameter reproducibility and the estimation stability of the RL and Prism-RL models. We then provide a real application result in the case study of pedestrian route choice, in which the Prism-RL model captures a positive utility effect of green presence on the streets.

We used the link-based formulation of the models and defined a prism for each destination. All models have been implemented in Python 3.6 on a machine with 14 core Intel Xeon W processors (2.5 GHz) and 64 GB of RAM. We implemented modeling, estimation, and validation by writing our own Python code, where for parameter search, we used the BFGS algorithm of the SciPy *optimize* module.

4.1. Numerical Experiments

We first report several experiments to show that the proposed Prism-RL model actually solves the numerical problem of the RL model. In the experiment, we use the Sioux-Falls network (Transportation Networks for Research Core Team, 2016) and define the utility function as

$$v(a|k) = \beta_{\text{len}} \text{Length}_a + \beta_{\text{cap}} \text{Capacity}_a - 10 \text{Uturn}_{a|k} \quad (12)$$

where Length_a is the length of link a , and Capacity_a is its capacity divided by 10000, which are available from the dataset (see Fig.A.5 in Appendix A)². We also add a negative and fixed u-turn penalty $\text{Uturn}_{a|k}$, which follows the previous studies of the RL model (e.g., Fosgerau et al., 2013). Here, as the main difference from the literature, we assume a possible positive effect of the capacity on the utility, i.e., β_{cap} can be greater than zero, while the length has a negative effect $\beta_{\text{len}} < 0$. Previous RL models have not been able to include a positive utility effect due to the numerical issue with the evaluation of the value function.

In the following experiments, we always use observations simulated by the RL model with a known vector of true parameters $\hat{\beta}$ and compare the estimation of the RL and Prism-RL models. We add the dimension of the choice stage to the observations for the estimation of the Prism-RL model, by the path translation we explained in Section 3.3, but the data nature does not change. We set the choice stage constraint $T = 15$ ³. Implementing a Monte-Carlo simulation, we generate 1000 observations for each origin-destination (OD) pair. We considered four destinations and six origins, i.e., 24 OD pairs in total. Note that we did not observe any path with a loop where a repeated link is considered a loop.

The summary of the experiments provided in this section is as follows.

- (1) We compare the estimation results of the RL and Prism-RL models. Two cases are tested:
 - (a) $\beta_{\text{cap}} < 0$ and (b) $\beta_{\text{cap}} > 0$. The objective of this experiment is to validate the potential

²Note that we use the variables of length and capacity just for the sake of convenience. We used only simulated observations for the Sioux Falls network case study, and the behavioral interpretations of the parameters are not of interest.

³We additionally tested the cases with $T = 10, 20, 30, 40$. The value of T did not affect the estimation result in the experiments, while the computational time approximately linearly increased with the increase in T .

of the Prism-RL model reproducing the true parameter of the RL model, even in the case in which a positive utility effect is considered.

- (2) We then investigate the estimation processes of the models by visualizing the parameter update histories. This experiment focuses on a case with $\beta_{\text{cap}} > 0$. We see how the RL model faces with the numerical issue during the estimation and how stable the estimation of the Prism-RL model is.

4.1.1. Parameter Reproducibility

This experiment validates the parameter reproducibility of the Prism-RL model. We divided the observations into 10 samples, each of which then has 2400 observations. The RL model and the Prism-RL model are estimated for every sample.

First, we set the true values of the parameters in (12) to $(\hat{\beta}_{\text{len}}, \hat{\beta}_{\text{cap}}) = (-1.5, -1.0)$, both of which are negative. Table 1 reports the estimation results. In this case, the two models returned the same results. All estimates and standard errors of the RL and Prism-RL models were exactly equal to four decimal places. As shown in Table 1, the true parameters are reproduced well and all estimates of the 10 samples are not significantly different from the true values at the 5% significance level. These results suggest that the Prism-RL model is able to sufficiently reproduce the parameters of the RL model. Note that the reason that the two models obtained the same results may be that the prism defined in this experiment sufficiently covered the distributional region of the RL model’s probability.

Table 1: Estimation results with the simulated observations. The true parameter values are $(\hat{\beta}_{\text{len}}, \hat{\beta}_{\text{cap}}) = (-1.5, -1.0)$. All estimates and standard errors of the RL and Prism-RL models were exactly equal to four decimal places.

Sample	β_{len}	std.err.	t-test	β_{cap}	std.err.	t-test
1	-1.529	0.028	1.059	-1.000	0.039	-0.009
2	-1.521	0.038	0.556	-0.978	0.054	-0.401
3	-1.506	0.028	0.201	-1.037	0.039	0.955
4	-1.509	0.051	0.174	-0.976	0.112	-0.213
5	-1.492	0.042	-0.181	-1.000	0.055	0.008
6	-1.468	0.032	-0.994	-0.996	0.040	-0.089
7	-1.504	0.034	0.107	-1.053	0.041	1.305
8	-1.514	0.026	0.535	-1.044	0.038	1.165
9	-1.538	0.028	1.372	-0.973	0.039	-0.698
10	-1.471	0.028	-1.003	-0.984	0.040	-0.403
Average	-1.505	0.034	0.183	-1.004	0.050	0.162

Next, we set the true parameters to $(\hat{\beta}_{\text{len}}, \hat{\beta}_{\text{cap}}) = (-2.5, 2.0)$ to include a positive utility effect. The initial parameter values were $(\hat{\beta}_{\text{len}}, \hat{\beta}_{\text{cap}}) = (-1.0, -1.0)$. Tables 2 and 3 report the estimation results of the RL model and the Prism-RL model, respectively. In this case, unlike the previous case where both parameters are negative, we observed a clear difference between the results of the two models. The RL model converged only once out of 10 samples. For the other 9 samples, the RL model diverged during the estimation process and failed to obtain the estimation results, even though the true value is a feasible solution of the RL model. In contrast, we succeeded in estimating the Prism-RL model for all samples. Like in the previous experiment, all estimates of the 10 samples are close to their true values, and they are not significantly different from their true values at the 5% significance level. These results validate that the Prism-RL model solves the numerical issue of the RL model regarding the evaluation of the value function and captures a positive variable effect on utility.

Table 2: Estimation results of the RL model with the simulated observations. The true parameter values are $(\hat{\beta}_{\text{len}}, \hat{\beta}_{\text{cap}}) = (-2.5, 2.0)$. For samples 1 and 3-10, we did not obtain results.

Sample	$\hat{\beta}_{\text{len}}$	std.err.	t-test	$\hat{\beta}_{\text{cap}}$	std.err.	t-test
2	-2.454	0.044	-1.028	1.984	0.085	0.192
1, 3-10	-	-	-	-	-	-

Table 3: Estimation results of the Prism-RL model with the simulated observations. The true parameter values are $(\hat{\beta}_{\text{len}}, \hat{\beta}_{\text{cap}}) = (-2.5, 2.0)$.

Sample	$\hat{\beta}_{\text{len}}$	std.err.	t-test	$\hat{\beta}_{\text{cap}}$	std.err.	t-test
1	-2.451	0.050	-0.972	1.982	0.037	0.481
2	-2.454	0.063	-0.724	1.984	0.051	0.318
3	-2.468	0.051	-0.620	1.976	0.037	0.654
4	-2.415	0.057	-1.499	1.954	0.036	1.275
5	-2.466	0.310	-0.111	1.943	0.258	0.221
6	-2.530	0.061	0.495	2.046	0.054	-0.847
7	-2.423	0.048	-1.597	1.950	0.051	0.997
8	-2.495	0.080	-0.062	2.012	0.039	-0.313
9	-2.511	0.112	0.101	2.040	0.064	-0.628
10	-2.455	0.049	-0.916	1.989	0.039	0.289
Average	-2.467	0.088	-0.591	1.988	0.067	0.245

4.1.2. Estimation Stability

To understand how the numerical issue of the RL model occurs during the estimation, we visualized its estimation process with different initial points. We used all observations at once for this experiment. Again, as in the previous experiment, we set the true values of the parameters in (12) to $(\hat{\beta}_{\text{len}}, \hat{\beta}_{\text{cap}}) = (-2.5, 2.0)$ including a positive utility effect. With three different initial points A $(-1, -1)$, B $(-3, 0)$, and C $(-4, 3)$, we compared the estimation processes of the RL and Prism-RL models (Fig.3a,b). When the initial point was A $(-4, 3)$, the RL and Prism-RL models both converged to the true value. However, in the other cases B and C, the RL model diverged during the estimation process (blue and green trajectories in Fig.3a), because the parameters were updated to values in the infeasible region. On the contrary, the Prism-RL model did not experience the numerical issue. Regardless of the initial point, the Prism-RL model converged to the true value. The process appeared stable and no fluctuation or update to the RL infeasible region was not observed (Fig.3b).

Moreover, we tested the estimation of the Prism-RL model with the initial point set to a value outside of the RL feasible region. The result is shown in Fig.3(c). We tested three initial values D $(1, 0)$, E $(0, 2)$ and F $(-1, 4)$, with which the RL model is infeasible due to the divergence of the value function. Fig.3(c) demonstrates that the Prism-RL model is feasible even with the parameters within the infeasible region of the RL model. This fact suggests the estimation stability of the Prism-RL model, since it is possible for the Prism-RL model to reach at the solution even if the parameter is updated outside of the RL feasible region during the estimation process.

4.2. Pedestrian Route Choice Application

To validate the usefulness of the Prism-RL model in real applications, we here present a case study of pedestrian route choice. It is assumed that, unlike other modes of transportation, pedestrians have more freedom in route choice behavior, and they may be affected by positive aspects (i.e., attractiveness) of streets. We use the GPS data collected through the Probe Person Survey, a complementary survey of the Sixth Tokyo Metropolitan Region Person Trip Survey (Ministry of Land, Infrastructure, Transport and Tourism of Japan, 2018). This study focuses on the pedestrian network of a mile square centered on the Kannai Station, Yokohama city, Japan (Fig.

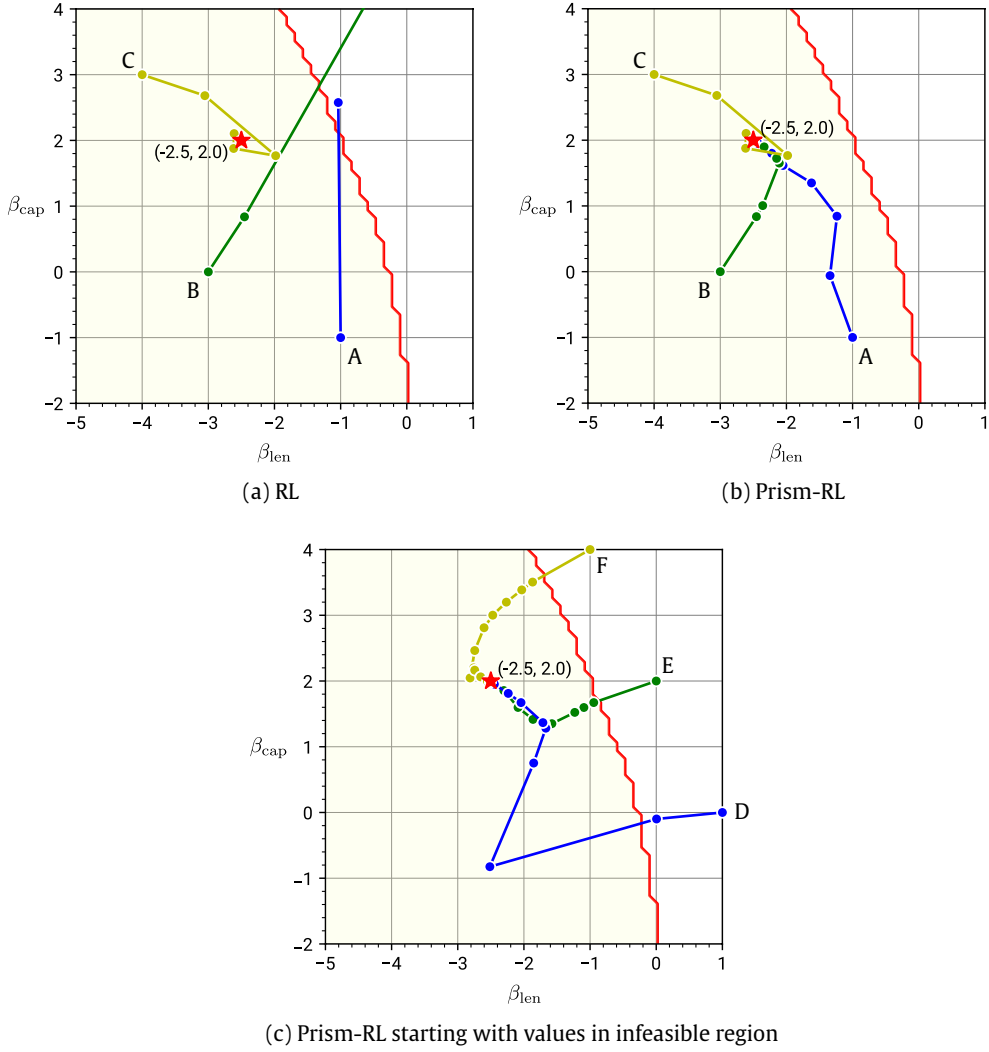


Figure 3: Parameter estimation processes of (a) RL model and (b) Prism-RL model tested with three different initial points A, B and C, and of (c) Prism-RL model with those in the infeasible region D, E and F. The yellowed area in the graph is the feasible region of the RL model.

B.6 in Appendix B). Yokohama is the second largest city in Japan by population. The Kannai district is popular for strolling; it is close to the sea and there are many places for refreshments, such as parks. The pedestrian network contains 724 nodes and 2398 links with 8434 link pairs. After map matching, we obtained 410 observed walking paths for 164 destinations of 159 unique pedestrians.

We analyze some characteristics of the observed paths in Appendix B, based on which we define the choice stage constraint T_d for destination d as

$$T_d \equiv \max_{n \in N_d} \{1.34 \times D^d(o_n), J_n\} \quad (13)$$

where N_d is the set of observations for d , and o_n is the observed origin for observation n . We use the 75 percentile value (≈ 1.34 , see Table B.5) for the detour rate multiplied with the minimum number of steps $D^d(o)$ between (o, d) . We compared it with the maximum number of steps observed \bar{J}_d for each destination and finally took the largest as T_d so that all observations satisfy the prism constraint.

We consider the following two specifications of the utility function:

$$v(a|k) = \beta_{\text{len}} \text{Length}_a + \beta_{\text{cross}} \text{Crosswalk}_a - 10 \text{Uturn}_{a|k}, \quad (14a)$$

$$v(a|k) = \beta_{\text{len}} \text{Length}_a + \beta_{\text{cross}} \text{Crosswalk}_a - 10 \text{Uturn}_{a|k} + \beta_{\text{green}} \text{Green}_a, \quad (14b)$$

where Length_a is the length (m/10) of link a , Crosswalk_a is the dummy variable of a being a crosswalk, and Green_a is the dummy variable of green presence on link a ⁴. Like in the experiments in the previous section, we fixed the coefficient of the uturn dummy variable to -10 and estimate the other coefficients β_{len} , β_{cross} , and β_{green} ⁵. We expect that the link length and crosswalks have negative utility effects, while the green existence has a positive utility effect on pedestrian route choice behavior. Therefore, we compare (14a) and (14b) in terms of model feasibility, as well as model fitting and interpretation.

Table 4 reports the estimation results. First, for specification (14a), we succeeded in estimating both the RL and Prism-RL models. Their estimates show similar mechanisms of pedestrian route choice behavior and are significantly different from zero at the 5% significance level. From the estimates signs, we found that pedestrians tend to walk paths with shorter lengths and avoid crosswalks, which meet our expectations.

By comparing, the Prism-RL model obtained a better log-likelihood value than the RL model. To further investigate this fact, we performed a hold-out validation. We randomly split the observations into estimation and validation samples with a ratio of 80% and 20% and prepared 10 sets of them. The choice stage constraint T is consistent with the case with all observations (13). Figure 4 shows the validation results. For all samples, the Prism-RL model outperforms the RL model in the sense of having a better log likelihood value. This difference comes from the path sets assumed by those models. The RL model implicitly considers all feasible paths, including infinite cyclic paths, while the Prism-RL model restricts such paths by the prism constraint. This validation result suggests that the prism-based approach is not only a way of solving the numerical issue regarding the value function of the RL model, but is also a more realistic description of route choice behavior.

Finally, we compare the estimation results of the two specifications (14a) and (14b). For (14b), which additionally includes the green dummy variable to (14a), we did not succeed in estimating the RL model although we have tried some initial points. On the contrary, the Prism-RL model did not experience the numerical problem, and we obtained the estimation result (the fifth column of Table 4)⁶. All estimates including β_{green} are significantly different from zero at the 5% significance level. Most importantly, the coefficient β_{green} of green presence was estimated with a positive sign, while the other two coefficients remained negative. This result indicates that pedestrians want to walk streets with green, which meet our expectation. We also perform the likelihood ratio test of the Prism-RL model with the specification (14b) against that with (14a):

$$-2(-1637.484 - (-1616.445)) = 42.078 > 3.84 = \chi_{0.05,1}^2 \quad (15)$$

which shows that model (14b) which includes a positive utility effect of green presence is preferred to (14a) with the 95% confidence level.

⁴If a street a has plants or trees on it or is along a park where some green is visible, Green_a is assumed as one. Otherwise, it is zero.

⁵The scale μ is normalized to one.

⁶Like the experiment in Section 4.1.2, the estimation result of the Prism-RL model did not depend on the initial point.

Table 4: Estimation results with the real observations. The second and third columns show the results for specification (14a), and the fourth and fifth columns for (14b). For specification (14b), we failed to estimate the RL model.

	RL (14a)	Prism-RL (14a)	RL (14b)	Prism-RL (14b)
β_{len}	-0.297	-0.245	-	-0.264
std.err.	0.008	0.007	-	0.014
t-test	-38.832	-37.264	-	-19.508
β_{cross}	-0.924	-0.774	-	-0.758
std.err.	0.075	0.171	-	0.082
t-test	-12.237	-4.517	-	-9.282
β_{green}			-	0.226
std.err.			-	0.036
t-test			-	6.317
LL	-1772.972	-1637.484	-	-1616.445
#paths	410	410	410	410

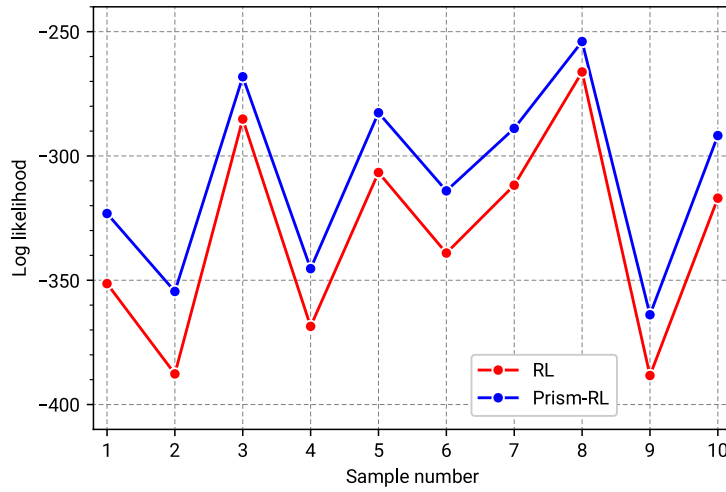


Figure 4: Validation results, the log likelihood values of the 10 hold-out samples, of the RL model (red) and the Prism-RL model (blue). The Prism-RL model is above the RL model for all samples.

4.3. Discussions

This section presented a set of numerical results, which validated the advantages of the Prism-RL model. The Prism-RL model solved the numerical issue of the RL model and enabled a stable estimation. It also succeeded in capturing positive variable effects on utility while retaining implicit path enumeration. In the real application, with the same specification of the utility function, the Prism-RL model got a higher goodness of fit than the RL model. This result implies that the Prism-RL model not only solves the numerical problem of the RL model, but it may also provide a more realistic description of route choice behavior by restricting unrealistic paths by the prism constraint.

In particular, for pedestrian route choice behavior, the definition of the set of paths is a difficult task due to the diversity of walking paths (we show an example in Figure B.7 in Appendix B). In such cases, classical approaches, i.e., route choice models with an explicit path generation algorithm, may not be useful because it is difficult to include diverse walking paths in the choice set. The unrestricted path set of the RL model also has the numerical problem discussed in this paper, as pedestrians are likely to be affected by some positive attributes of the streets in route choice behavior. The Prism-RL model addresses these two challenges, which is shown in the real case study of a pedestrian network.

Some readers may think that the effect of green presence on streets can be captured by considering the opposite effect, i.e., the negative utility of green absence. However, unlike in path-based route choice models, a dummy variable in the RL model does not necessarily have a symmetric effect on the choice probability (see Proposition 1 in Appendix D). As such, incorporating positive utilities may be preferable for behavioral interpretation and policy design, given that many urban design projects expect such street designs to work as attractiveness and make cities more walkable (e.g., Mehta, 2008; Mueller et al., 2020). Although this study focuses on the methodology and showed the pedestrian case study as an example to validate the proposed model, including only a dummy variable of green presence as positive utility is not enough to understand pedestrian route choice behavior. As well as observing and estimating the continuous effect of green volume, using the present model for a more detailed analysis of pedestrian route choice, such as more sophisticated model specifications and inter-regional comparison are interesting topics for future research.

The numerical examples used the original topology of the network to define the choice stage, which implies that we restrict the feasible path set by the maximum link number. According to the definition, we used the detour rate that is based on the number of links contained in the path. However, by changing the definition of choice stage, the Prism-RL model can take another type of constraint, such as the maximum length or time of paths (see Oyama and Hato, 2019, for the detail). The prism constraint defined based upon a specific variable such as travel distance or time may be easier to behaviorally interpret, but they require network editing (i.e., link splitting into unit length), which increases the number of states and makes the computation inefficient. By contrast, the prism constraint based on the number of links, which this study used, does not depend on a specific variable or require network editing. Furthermore, when the network has cycles consisting of very short links, the constraint of the maximum link number in a path should be able to restrict such cyclic route choice behavior.

Note that even though the Prism-RL model is executable in a reasonable time, it requires more computational effort than the RL model, and the computational time depends on the definition of choice stage constraint (see Appendix C). This is because the linear system (3) of the RL model, which can be efficiently computed, is not available for the Prism-RL model. Nevertheless, the advantage of (9) is its independence of whether the model is linear or nonlinear (Oyama and Hato, 2019). Therefore, the Prism-RL model may be faster than existing nonlinear RL models that have to solve the convergence of the value function typically by the value iteration (e.g., Mai et al., 2015). The application of the present method to nonlinear models and its comparison with existing models would be an interesting future step.

5. Concluding Remarks

This study proposed a prism-constrained recursive logit (Prism-RL) model that solves the numerical problem of the RL model and enables its stable estimation. The Prism-RL model implicitly restricts the feasible path set by the prism constraint based on the state-extended network by choice stages. While retaining the implicit path enumeration, it is also possible to define the set of path alternatives in a data-oriented manner, such as using the observed detour rates. This enables a more realistic description of route choice behavior.

As a result of the application, we obtained two important achievements. First, the Prism-RL model got a higher goodness of fit than the RL model, which was well demonstrated by the hold-out validation. Second and most importantly, we succeeded in capturing a variable with a positive utility effect. In the real application in a pedestrian network, we found that the presence of green acts as an attraction in pedestrian route choice behavior. It has not been possible to capture such a positive utility effect with the previous RL models due to the numerical issue regarding the value function evaluation.

Around the world, urban design projects are recently planned to make better places in city centers where many people visit and enjoy walking (e.g., [Mueller et al., 2020](#)). To properly evaluate the impacts of such projects, it is not enough to capture only negative utility effects. It has been necessary to develop a method that is able to analyze the attractiveness having positive effects on pedestrians' behavior, and our proposed method can also be considered as a significant contribution in such a context.

Given the way of solving the numerical issue of the RL model, there are a number of open and potentially valuable research directions for further study. Recursive modeling of behavior is a general framework, and its application is not limited to route choice behavior. Modeling of trip chaining behavior (e.g., [Kitamura, 1984](#)), i.e., a sequence of destination choices, is a particular application in which we need to adequately evaluate the attractiveness of destinations. The Prism-RL model will be useful for such a case, and this research direction seems appealing. Network design problems with positive impacts can be formulated by using the Prism-RL model as a demand-side simulation tool. Possible model extensions include the incorporation of uncertainty or travelers' heterogeneity in constraints, applications to nonlinear models, and algorithm developments to speed up the estimation.

Acknowledgements

This research was supported by JSPS KAKENHI Grant Number 20K14899. The data for the case study was collected through a Probe Person (PP) survey, complementary survey of the Sixth Tokyo Metropolitan Region Person Trip (PT) Survey.

Appendix A. Sioux Falls Network Data

Figure [A.5](#) shows the Sioux Falls network, where (a) and (b) map the values of link length and link capacity. Note that the link lengths are equal to the free-flow link costs in the provided data ([Transportation Networks for Research Core Team, 2016](#)), which is why the length variable is not consistent with the visual length of Figure [A.5](#).

Appendix B. Pedestrian Network and Route Choice Data

Figure [B.6](#) shows the pedestrian network for the real application, which includes street data within a mile square centered on the Kannai station, Yokohama city, Japan. The dummy variables $Crosswalk_a$ and $Green_a$ are also mapped. The Kannai district has many streets with visible green. Note that we obtained the original network data from [OpenStreetMap contributors \(2017\)](#) using the Python library OSMnx ([Boeing, 2017](#)), on which we added the street variables.

Figure [B.7](#) exhibits four examples of observed walking paths with high detour rates. We find that pedestrians walk a variety of paths, sometimes taking a large detour. We also observe that, in the path (b), the upper right one, the pedestrian takes a path passing through streets with green.

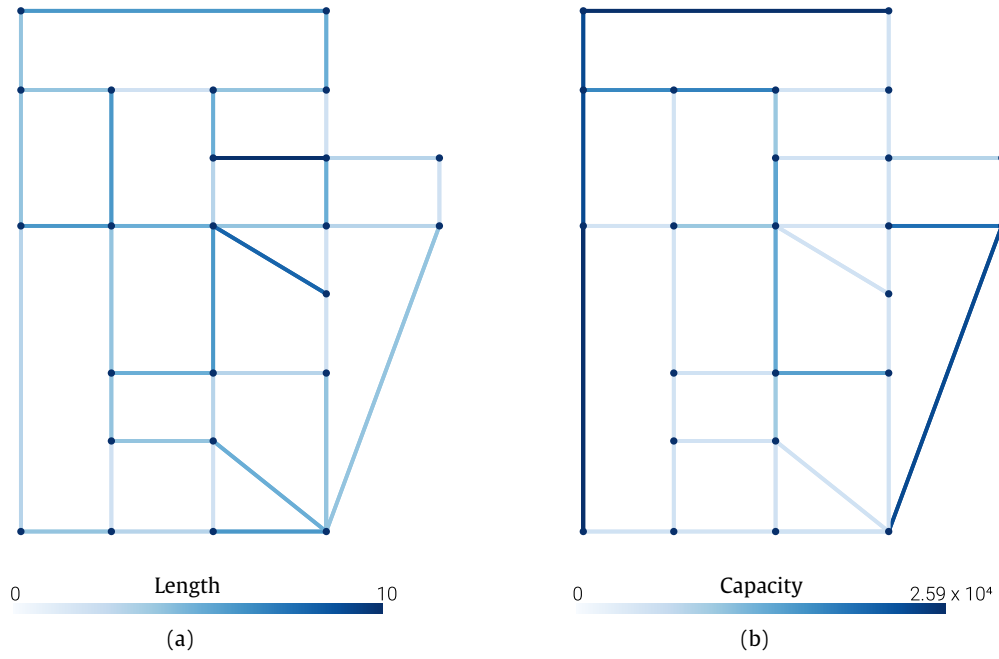


Figure A.5: Link variables in the Sioux Falls network: (a) length, (b) capacity. Deep colored lines indicate links with larger magnitude of variables.

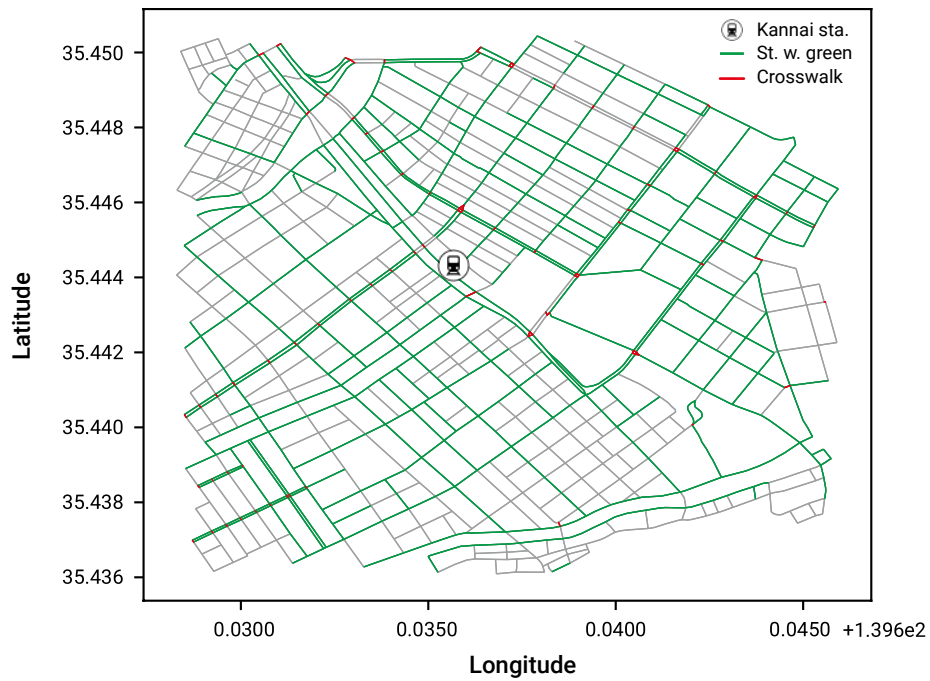


Figure B.6: Pedestrian network for real application. The area is a mile square centered on the Kannai station. Green lines indicate streets with green, and red lines are crosswalks.

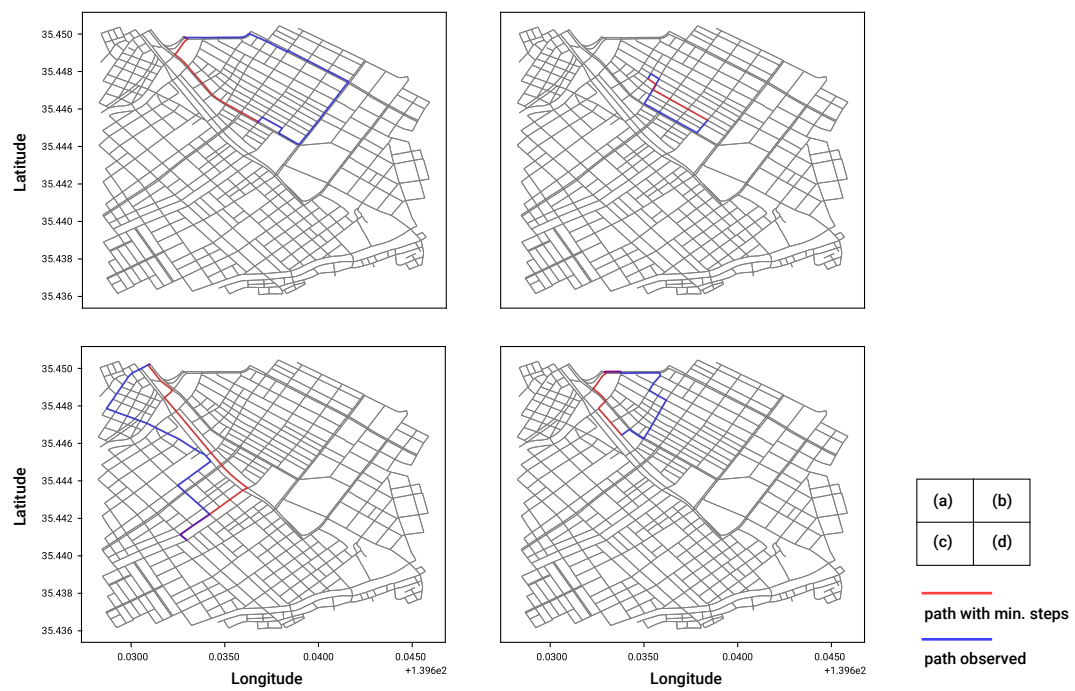


Figure B.7: Examples of observed detour walking paths. Blue paths are the observed paths, and red paths are paths with minimum steps between the observed OD pairs.

Figure B.8 is the plot of the detour characteristics of the observed walking trips, and Table B.5 reports the statistics of the observed detour rates, where we defined a detour rate as the number of steps observed (links) divided by the minimum number of steps. The detour rates of 75% of the observed paths are below $4/3 \approx 1.34$. We used this value as well as the maximum step number for the decision of the choice stage constraint T_d for each destination d , as Eq.(13).

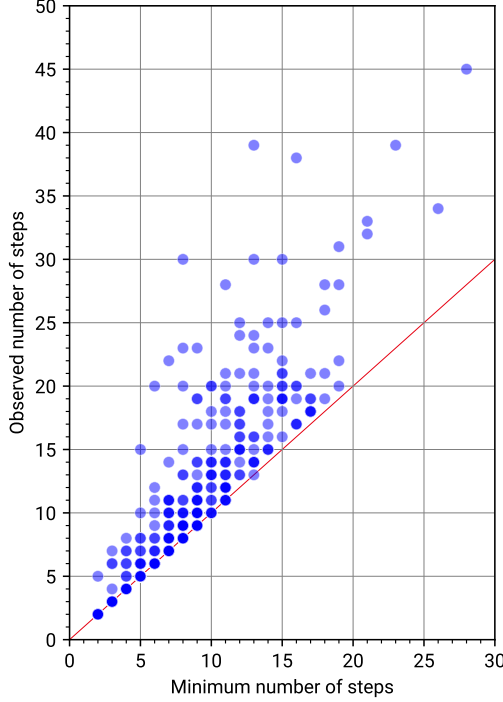


Figure B.8: Plot of detour characteristics of the observed paths. The x-axis is the minimum step for each observed OD pair, and the y-axis is the steps actually used. Deep colors mean that the points are observed many times. The red line is the identity line.

Table B.5: Statistics of detour rates, or the observed number of steps divided by the minimum number of steps.

Count	Mean	Std.	Min.	25%	50%	75%	Max.
410	1.24	0.39	1.00	1.00	1.08	1.33	3.75

Appendix C. Computational time for estimation

Table C.6 reports the estimation time for the Sioux Falls network experiment, the case with $(\hat{\beta}_{\text{len}}, \hat{\beta}_{\text{cap}}) = (-1.5, -1.0)$, in Section 4.1.1. The Prism-RL model requires more computational time than the RL model, and its increase is approximately linear in the choice stage constraint T .

Table C.7 reports the estimation time for the real application in Section 4.2. The RL model is very fast because its value function can be efficiently computed by solving (3). The Prism-RL model requires more computational effort than the RL model, although it is still feasible in the real-size network. For specification (14b), we did not obtain the result of the RL model due to the numerical issue regarding positive utilities.

Table C.6: Estimation time for the Sioux Falls network experiment. The reported values are the average times over 10 samples.

Model	RL	Prism-RL				
T	-	10	15	20	30	40
CPU time (sec.)	0.860	1.679	2.851	4.015	6.736	8.922

Table C.7: Estimation time for the real application. The reported values are the average times over the 10 hold-out samples.

Model	RL (14a)	Prism-RL (14a)	RL (14b)	Prism-RL (14b)
CPU time (sec.)	36.712	386.240	N/A	692.525

Appendix D. Asymmetric effect of dummy variables

Proposition 1. Consider two utility specifications $v(a|k) = v_c(a|k) + \beta x_{a|k}$ and $v'(a|k) = v_c(a|k) - \beta(1 - x_{a|k})$ where $x_{a|k}$ is a dummy variable taking one or zero. For the choice probability \mathbf{P} of the RL model, $\mathbf{P}(v) = \mathbf{P}(v')$ does not necessarily hold.

Proof. One can easily find a counterexample to $\mathbf{P}(v) = \mathbf{P}(v')$. Consider the toy network of Figure D.9 and utility functions $v(a|k) = x_{a|k}$ and $v'(a|k) = -(1 - x_{a|k})$, i.e., $v_c(a|k) = 0$ and $\beta = 1$, for simplicity. It is assumed that $x_{a_2|k} = x_{a_3|a_2} = 1$ and $x_{a|k} = 0$ for the others. Then, the RL model returns $p(a_2|k, v)/p(a_1|k, v) = e^2$ and $p(a_2|k, v')/p(a_1|k, v') = e$, which indicates $\mathbf{P}(v) \neq \mathbf{P}(v')$ in this example. \square

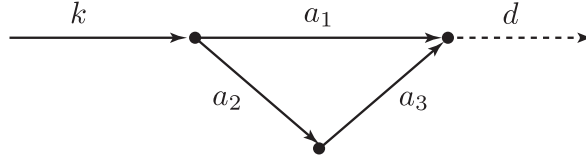


Figure D.9: Toy network with four links and the dummy destination link.

References

- Akamatsu, T., 1996. Cyclic flows, Markov process and stochastic traffic assignment. *Transportation Research Part B: Methodological* 30, 369–386.
- Akamatsu, T., 1997. Decomposition of Path Choice Entropy in General Transport Networks. *Transportation Science* 31, 349–362.
- Baillon, J.B., Cominetti, R., 2008. Markovian traffic equilibrium. *Mathematical Programming* 111, 33–56.
- Boeing, G., 2017. Osmnx: New methods for acquiring, constructing, analyzing, and visualizing complex street networks. *Computers, Environment and Urban Systems* 65, 126–139.
- Fosgerau, M., Frejinger, E., Karlstrom, A., 2013. A link based network route choice model with unrestricted choice set. *Transportation Research Part B: Methodological* 56, 70–80.

- de Freitas, L.M., Becker, H., Zimmermann, M., Axhausen, K.W., 2019. Modelling intermodal travel in switzerland: A recursive logit approach. *Transportation Research Part A: Policy and Practice* 119, 200–213.
- Gao, Y., Schmöcker, J.D., 2021. Estimation of walking patterns in a touristic area with wi-fi packet sensors. *Transportation Research Part C: Emerging Technologies* 128, 103219.
- Hägerstrand, T., 1970. What about people in regional science? *Regional Science Association* 24.
- Kitamura, R., 1984. Incorporating trip chaining into analysis of destination choice. *Transportation Research Part B: Methodological* 18, 67–81.
- Kivimäki, I., Van Moorter, B., Panzacchi, M., Saramäki, J., Saelens, M., 2020. Maximum likelihood estimation for randomized shortest paths with trajectory data. *Journal of Complex Networks* 8, cnaa024.
- Mai, T., 2016. A method of integrating correlation structures for a generalized recursive route choice model. *Transportation Research Part B: Methodological* 93, 146–161.
- Mai, T., Bastin, F., Frejinger, E., 2018. A decomposition method for estimating recursive logit based route choice models. *EURO Journal on Transportation and Logistics* 7, 253–275.
- Mai, T., Fosgerau, M., Frejinger, E., 2015. A nested recursive logit model for route choice analysis. *Transportation Research Part B: Methodological* 75, 100–112.
- Mai, T., Yu, X., Gao, S., Frejinger, E., 2021. Route choice in a stochastic time-dependent network: the recursive model and solution algorithm. *Transportation Research Part B: Methodological* 151, 42.
- Mehta, V., 2008. Walkable streets: pedestrian behavior, perceptions and attitudes. *Journal of Urbanism* 1, 217–245.
- Ministry of Land, Infrastructure, Transport and Tourism of Japan, 2018. The Sixth Tokyo Metropolitan Region Person Trip Survey.
- de Moraes Ramos, G., Mai, T., Daamen, W., Frejinger, E., Hoogendoorn, S., 2020. Route choice behaviour and travel information in a congested network: Static and dynamic recursive models. *Transportation Research Part C: Emerging Technologies* 114, 681–693.
- Mueller, N., Rojas-Rueda, D., Khreis, H., Cirach, M., Andrés, D., Ballester, J., Bartoll, X., Daher, C., Deluca, A., Echave, C., et al., 2020. Changing the urban design of cities for health: The superblock model. *Environment international* 134, 105132.
- OpenStreetMap contributors, 2017. Planet dump retrieved from <https://planet.osm.org> . <https://www.openstreetmap.org>.
- Oyama, Y., Hara, Y., Akamatsu, T., 2022. Markovian traffic equilibrium assignment based on network generalized extreme value model. *Transportation Research Part B: Methodological* 155, 135–159.
- Oyama, Y., Hato, E., 2016. Pedestrian activity model based on implicit path enumeration, in: *Proceedings of the 21st International Conference of Hong Kong for Transportation Studies (HKSTS)*, pp. 331–338.

- Oyama, Y., Hato, E., 2017. A discounted recursive logit model for dynamic gridlock network analysis. *Transportation Research Part C: Emerging Technologies* 85, 509–527.
- Oyama, Y., Hato, E., 2018. Link-based measurement model to estimate route choice parameters in urban pedestrian networks. *Transportation Research Part C: Emerging Technologies* 93, 62–78.
- Oyama, Y., Hato, E., 2019. Prism-based path set restriction for solving markovian traffic assignment problem. *Transportation Research Part B: Methodological* 122, 528–546.
- Rust, J., 1987. Optimal replacement of gmc bus engines: An empirical model of harold zurcher. *Econometrica: Journal of the Econometric Society* , 999–1033.
- Saerens, M., Achbany, Y., Fouss, F., Yen, L., 2009. Randomized shortest-path problems: Two related models. *Neural Computation* 21, 2363–2404.
- Transportation Networks for Research Core Team, 2016. *Transportation Networks for Research*. URL: <https://github.com/bstabler/TransportationNetworks>. accessed: July 13, 2016.
- van Oijen, T.P., Daamen, W., Hoogendoorn, S.P., 2020. Estimation of a recursive link-based logit model and link flows in a sensor equipped network. *Transportation Research Part B: Methodological* 140, 262–281.
- Ziebart, B.D., Maas, A.L., Bagnell, J.A., Dey, A.K., et al., 2008. Maximum entropy inverse reinforcement learning., in: *Aaai*, Chicago, IL, USA. pp. 1433–1438.